

Full characterization of biphotons with a generalized quantum interferometer

Baihong Li(李百宏)^{1,*} Changhua Chen(陈昌花)¹, Boxin Yuan(袁博欣)¹,

Ruifang Dong(董瑞芳)^{2,†} Shougang Zhang(张首刚)², and Rui-Bo Jin(金锐博)^{3‡}

¹ School of Physics and Information Science, Shaanxi University of Science and Technology, Xi'an 710021, China

² Key Laboratory of Time and Frequency Primary Standards,

National Time Service Center, Chinese Academy of Sciences, Xi'an 710600, China and

³ Hubei Key Laboratory of Optical Information and Pattern Recognition,

Wuhan Institute of Technology, Wuhan 430205, China

Entangled photons (biphotons) in the time-frequency degree of freedom play an important role in both foundational physics and advanced quantum technologies. How to fully characterize them becomes a key scientific issue. Here, by introducing a frequency shift in one arm of interferometers, we propose theoretically a generalized combination quantum interferometer which allows simultaneous measurement of the amplitude and phase of biphotons associated with both frequency sum and difference in a single interferometer, performing the full tomography of biphotons. The results are compared with the Hong-Ou-Mandel and N00N state interferometers which only allows to perform the partial tomography of biphotons, and an experimental feasibility is also discussed. This provides an alternative method for full characterization of an arbitrary two-photon state with exchange symmetry and might become a useful tool for high-dimensional quantum information processing.

I. INTRODUCTION

Entangled photon sources in the time-frequency degree of freedom plays an important role in both foundational physics and advanced quantum technologies such as high-dimensional quantum information processing [1–3]. Because the high-dimensional information can be naturally encoded in time and frequency degree of freedom, such entangled sources have a potential in improving the robustness and key rate of quantum communication protocols [4–6], quantum enhanced sensing [7] and achieving more efficient and error-tolerant quantum computation [8]. These require well-characterized sources and how to fully characterize them becomes a key scientific issue.

A direct way of characterizing the spectrum of entangled photon pairs (biphotons) is to measure the joint spectral intensity (JSI) which gives the probability of detecting the photons with given frequencies [9] and the joint temporal intensity (JTI), which gives the probability of detecting the photons at given arrival times [10, 11]. Taken together, joint measurements in both frequency and time have enabled partial characterization of entangled ultrafast photon pairs, but still cannot provide the full two-photon state [11]. An indirect way is quantum Fourier-transform spectroscopy established by extended Wiener–Khintchin theorem [12–14], where the spectral information of entangled light can be extracted by making a Fourier transform on its time-domain interferograms obtained from the Hong-Ou-Mandel(HOM) interferometer [15, 16], the N00N state interferometer [17–19] or their combination [20].

However, these two ways are both insensitive to phase and hence cannot reveal the phase information of biphotons [11, 21]. To obtain the phase information of biphotons, some efforts has been made based on the phase retrieval algorithm that widely used in classical ultrafast optics [22, 23]. Recently, Davis et.al [24] demonstrated a technique to determine the full quantum state of biphotons based on electro-optic shearing interferometry. Some related review articles can be found in Ref. [25, 26]. Later, N. Fabre [27] proposed a generalized HOM interferometer which allows the measurement of the amplitude and phase of biphotons associated with frequency difference for biphotons having a joint spectral amplitude (JSA) of any symmetry, and a generalized N00N state interferometer allows the measurement of amplitude and phase of biphotons associated with frequency sum only for symmetric JSA and frequency difference only for antisymmetric JSA. However, it is impossible to obtain fully the amplitude and phase of biphotons associated with both frequency difference and sum in these two interferometers.

In this paper, we extend the combination interferometer we proposed recently in [20] to a generalized one by introducing a frequency shift in one arm of the interferometer. Through comparing it with the generalized HOM and N00N state interferometers, it is found that with the generalized combination interferometer, it is possible to measure the amplitude and phase of biphotons associated with both frequency difference and sum for symmetric JSA or antisymmetric JSA in a single interferometer, performing the full tomography of biphotons. This may provide

* li-baihong@163.com

† dongruifang@ntsc.ac.cn

‡ jin@wit.edu.cn

an alternative method for full characterization of an arbitrary two-photon state with exchange symmetry and might become a useful tool in high-dimensional quantum information processing.

The rest of the paper is organized as follows. In section II, we describe the generalized HOM interferometer and discuss the possibility on the measurement of the amplitude and phase of biphotons associated with frequency difference for any symmetric JSA. In section III, we describe the generalized N00N interferometer and discuss the possibility on the measurement of the amplitude and phase of biphotons associated with frequency sum for symmetric JSA and frequency difference for antisymmetric JSA. In section IV, we describe the generalized combination interferometer and discuss the possibility on the measurement of the amplitude and phase of biphotons associated with both frequency difference and sum for symmetric JSA or antisymmetric JSA. Section V compares the results obtained with three generalized interferometers and discusses the experimental feasibility on the measurement of amplitude and phase of biphotons with these generalized interferometers. Section VI summarizes the results and concludes the paper.

II. GENERALIZED HOM INTERFEROMETER

The setup of a generalized HOM interferometer is shown in Fig. 1(a), where a frequency shift is introduced in the idler arm. The biphotons are generated by the spontaneous parametric down-conversion (SPDC). The coincidence count rates between two detectors D1 and D2 as functions of time delay τ and the frequency shift μ for the generalized HOM interferometer can be expressed as

$$R(\tau, \mu) = \frac{1}{2} \int_0^\infty \int_0^\infty d\omega_s d\omega_i \left| f(\omega_i + \mu, \omega_s) e^{-i\omega_s \tau} - f(\omega_s, \omega_i + \mu) e^{-i\omega_i \tau} \right|^2. \quad (1)$$

where $f(\omega_s, \omega_i)$ is the JSA of the signal(s) and idler(i) photons. In general, the JSA can not be factorized as a product of $f(\omega_s)$ and $f(\omega_i)$. However, it can be expressed in terms of collective coordinate ω_+ and ω_- and generally be decomposed as follows [21, 27],

$$f(\omega_s, \omega_i) = f_+(\omega_+) f_-(\omega_-). \quad (2)$$

where $\omega_\pm = (\omega_s \pm \omega_i)/2$, and f_+ can be used to model the energy conservation of the SPDC process and it depends on the spectral profile of the pump. f_- is the phase-matching function, which can have various forms depending on the considered nonlinear crystal and the method to achieve phase matching. Because the exchange between ω_s and ω_i does not affect the sum of ω_+ , and thus the exchange symmetry of f_+ . However, this is not the case for the difference of ω_- , where the exchange between ω_s and ω_i results in the change of the exchange symmetry of f_- , i.e., $f(\omega_i, \omega_s) = -f_+(\omega_+) f_-(\omega_-)$.

As derived in Appendix A, Eq.(1) can be further simplified as

$$R(\tau, \mu) = \frac{1}{2} \left(1 - \text{Re}[W_-(\tau, \mu/2)] \right). \quad (3)$$

where

$$W_-(\tau, \mu/2) = \int d\omega_- f_-(\mu/2 - \omega_-) f_-^*(\mu/2 + \omega_-) e^{-i2\omega_- \tau}. \quad (4)$$

is the chronocyclic Wigner distribution of the phase matching function f_- [28, 29]. The cut of the Wigner distribution at $\mu = 0$ corresponds to the original HOM interference result. When $R(\tau, \mu) > 1/2$, the chronocyclic Wigner distribution is negative, which is an entanglement witness [30]. Note that since the HOM interference always depends on the frequency difference between the signal and the idler photons whatever the JSA is symmetric, antisymmetric or anyonic [12, 20, 27], it only allows to measure the amplitude of biphotons associated with the frequency difference for any symmetric JSA. However, the generalized HOM interferometer is a measurement of the displaced parity operator of only the phase matching part of the full JSA [31]. The chronocyclic Wigner distribution $W_-(\tau, \mu)$ can be obtained from the coincidence probability measured with the HOM interferometer at different frequency shifts μ . With the generalized HOM interferometer, it is possible to measure the real part of the chronocyclic Wigner distribution $W_-(\tau, \mu)$ associated with frequency difference for any symmetric JSA (Eq.(3)). If one introduces a phase $e^{i\pi/2}$ in one of the arms of the generalized HOM interferometer, then the imaginary part of W_- is measured. Experimentally, such a phase can be realized with a quarter wave plate. Once the real and imaginary parts are obtained, assuming that $f_-(0) = 0$, the following reconstruction formula can be used:

$$f_-^*(\mu) = \frac{1}{f_-(0)} \int W_-(\tau, \mu) d\tau, \quad (5)$$

to perform the full tomography of f_- . This has been shown schematically in the right part of Fig.1(a).

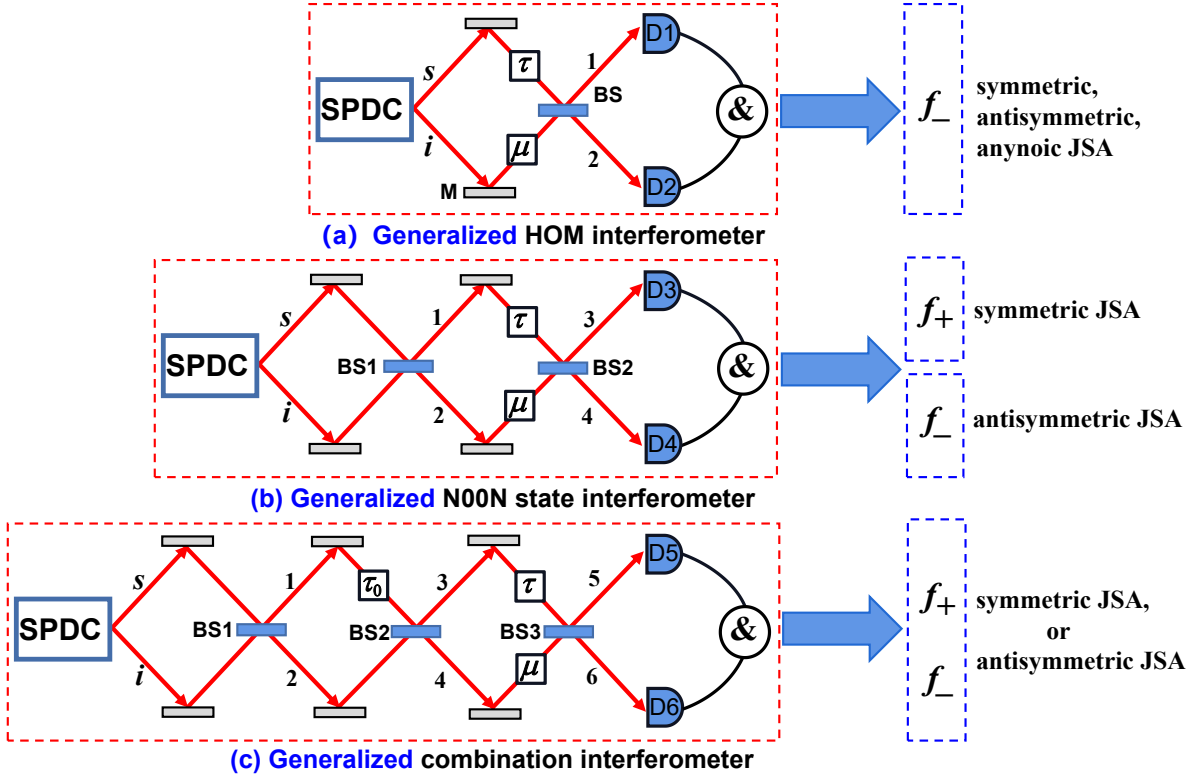


FIG. 1. (a) Generalized HOM interferometer, allowing the measurement of the amplitude and phase of f_- for any symmetric JSA. (b) Generalized N00N state interferometer, which allows the measurement of the amplitude and phase of f_+ for symmetric JSA and of f_- for antisymmetric JSA. (c) Generalized combination interferometer, allowing the measurement of the amplitude and phase of both f_+ and f_- for symmetric or antisymmetric JSA. τ represents the time delay between two arms of interferometers, and μ the frequency shift. If there is no frequency shift μ in above interferometers, i.e., $\mu = 0$, they would come back to the original ones and only allow the measurement of the amplitude of the corresponding f . M:Mirror, BS: beamsplitter, D: detector, & : coincidence measurement.

III. GENERALIZED N00N STATE INTERFEROMETER

The setup of a generalized N00N state interferometer is shown in Fig. 1(b), where a frequency shift is introduced in the path 2. The coincidence count rates between two detectors D3 and D4 as functions of the time delay τ and the frequency shift μ for the generalized N00N state interferometer can be expressed as

$$R(\tau, \mu) = \frac{1}{2} \int \int d\omega_s d\omega_i \left| f(\omega_s, \omega_i, \mu) (e^{-i(\omega_s + \mu)\tau} + 1) (e^{-i(\omega_i + \mu)\tau} + 1) + f(\omega_i, \omega_s, \mu) (e^{-i(\omega_i + \mu)\tau} - 1) (e^{-i(\omega_s + \mu)\tau} - 1) \right|^2. \quad (6)$$

Note that the N00N state is $|2002\rangle = |2, 0\rangle + |0, 2\rangle$ in Fig. 1(b), and the N00N state interferometer also called Mach-Zehnder interferometer of biphotons in some Refs.[27, 32]. The specific expression of Eq.(6) depends on the exchange symmetry of the JSA. If the JSA is symmetric, i.e., $f(\omega_s, \omega_i) = f(\omega_i, \omega_s)$, we can simplify Eq.(6) as (see Appendix B)

$$R_S(\tau, \mu) = \frac{1}{2} \left(1 + \text{Re}[F_+(\mu, 2\tau)] \right). \quad (7)$$

where F_+ is the short-time Fourier transform (STFT) of the function f_+ defined as

$$F_+(\mu, 2\tau) = \int d\omega_+ f_+(\omega_+) f_+^*(\omega_+ + \mu) e^{i(2\omega_+ + \mu)\tau}. \quad (8)$$

If the JSA is antisymmetric, i.e., $f(\omega_s, \omega_i) = -f(\omega_i, \omega_s)$, we can further simplify Eq.(6) as (see Appendix B)

$$R_A(\tau, \mu) = \frac{1}{2} \left(1 + \text{Re}[e^{-i\mu\tau/2} F_-(\mu, 2\tau)] \right). \quad (9)$$

where F_- is the STFT of the function f_- defined as

$$F_-(\mu, 2\tau) = \int d\omega_- f_-(\omega_-) f_-^*(\omega_- + \mu) e^{-i2\omega_- \tau}. \quad (10)$$

The additional phase factor $e^{-i\mu\tau/2}$ in Eq.(9) stems from the symmetric time-frequency displacement operator $\hat{D}(\mu, \tau)$ [27],

$$\chi_\psi(\mu, \tau) = \langle \psi | \hat{D}(\mu, \tau) | \psi \rangle = e^{-i\mu\tau/2} \int d\omega_- f_-(\omega_- - \mu) f_-^*(\omega_-) e^{i\omega_- \tau}. \quad (11)$$

where $\hat{D}(\mu, \tau) = e^{-i\mu\tau/2} \int d\omega e^{-i\omega\tau} |\omega + \mu\rangle \langle \omega|$ [31].

Note that since the N00N state interference depends on the frequency sum between the signal and the idler photons for symmetric JSA, but the frequency difference for antisymmetric JSA [12, 20, 27], it only allows to measure the amplitude of biphotons associated with the frequency sum for symmetric JSA or frequency difference for antisymmetric JSA. With the generalized N00N state interferometer, it is possible to measure the real part of the STFT of f_+ associated with frequency sum for symmetric JSA (Eq.(7)) and the STFT of f_- associated with frequency difference for antisymmetric JSA (Eq.(9)). If one introduces a phase $e^{i\pi/2}$ in one of the arms inside the generalized N00N state interferometer, then the imaginary part of the STFT of f_\pm is measured. Once the real and imaginary parts are obtained, assuming that $f_\pm(0) = 0$, the following reconstruction formula can be used:

$$f_\pm^*(\mu) = \frac{1}{f_\pm(0)} \int F_\pm(\mu, \tau) d\tau, \quad (12)$$

to perform the full tomography of f_+ for symmetric JSA and f_- for antisymmetric JSA. This has been shown schematically in the right part of Fig.1(b).

IV. GENERALIZED COMBINATION INTERFEROMETER

The setup of a generalized combination interferometer is shown in Fig. 1(c), where a frequency shift is introduced in the path 4. The coincidence count rates between two detectors D5 and D6 as functions of the time delay τ , τ_0 and the frequency shift μ can be expressed as

$$R(\tau_0, \tau, \mu) = \frac{1}{64} \int \int d\omega_s d\omega_i \times \left| f(\omega_s, \omega_i, \mu) (e^{-i\omega_s \tau_0} e^{-i(\omega_s + \mu)\tau} + e^{-i\omega_s \tau_0} + e^{-i(\omega_s + \mu)\tau} - 1) (e^{-i\omega_i \tau_0} e^{-i(\omega_i + \mu)\tau} - e^{-i\omega_i \tau_0} - e^{-i(\omega_i + \mu)\tau} - 1) + f(\omega_i, \omega_s, \mu) (e^{-i\omega_i \tau_0} e^{-i(\omega_i + \mu)\tau} + e^{-i(\omega_i + \mu)\tau} - e^{-i\omega_i \tau_0} + 1) (e^{-i\omega_s \tau_0} e^{-i(\omega_s + \mu)\tau} - e^{-i(\omega_s + \mu)\tau} + e^{-i\omega_s \tau_0} + 1) \right|^2. \quad (13)$$

Also, the specific expression of Eq.(13) depends on the exchange symmetry of the JSA. If the JSA is symmetric, i.e., $f(\omega_s, \omega_i) = f(\omega_i, \omega_s)$, we can simplify Eq.(13) as (see Appendix C)

$$R_S(\tau_0, \tau, \mu) = \frac{1}{2} \left(1 - \frac{1}{2} \text{Re}[e^{-i\mu\tau/2} F_-(\mu, 2\tau)] \text{Re}[P_+(\tau_0)] - \frac{1}{2} \text{Re}[F_+(\mu, 2\tau)] - \frac{1}{2} \text{Re}[e^{-i\mu\tau/2} F_-(\mu, 2\tau)] + \frac{1}{4} \text{Re}[F_+(\mu, 2(\tau + \tau_0))] + \frac{1}{4} \text{Re}[F_+(\mu, 2(\tau - \tau_0))] \right). \quad (14)$$

where F_+ and F_- are the STFT of the function f_+ and f_- , respectively, as defined in Eq.(8) and Eq.(10). $P_+(\tau_0)$ is defined as

$$P_+(\tau_0) = \int d\omega_+ f_+(\omega_+) e^{-i(2\omega_+ + 2\mu)\tau_0}. \quad (15)$$

Again, the additional phase factor $e^{-i\mu\tau/2}$ in Eq.(14) stems from the symmetric time-frequency displacement operator \hat{D} defined in Eq.(11). If we take f_+ as a Gaussian function, i.e., $f_+(\omega_+) = \exp(-\omega_+^2/4\sigma_+^2)$, where σ_+ denote the linewidth of the pump pulse, then $\text{Re}[P_+(\tau_0)] \sim \cos(\mu\tau) e^{-\sigma_+^2 \tau_0^2/4}$. The last two terms in Eq.(14) correspond to two identical interferograms centered at $\pm 2\tau_0$. If $\tau_0 < 1/\sigma_+$, these two interferograms will gradually overlap and become

fully indistinguishable as τ_0 decreases to be zero. Thus, if one would like to distinguish these two interferograms, τ_0 must be much larger than the inverse linewidth $1/\sigma_+$ [20], resulting in $Re[P_+(\tau_0)] \sim 0$. So, we have

$$R_S(\tau_0, \tau, \mu) = \frac{1}{2} \left(1 - \frac{1}{2} Re[F_+(\mu, 2\tau)] - \frac{1}{2} Re[e^{-i\mu\tau/2} F_-(\mu, 2\tau)] \right. \\ \left. + \frac{1}{4} Re[F_+(\mu, 2(\tau + \tau_0))] + \frac{1}{4} Re[F_+(\mu, 2(\tau - \tau_0))] \right). \quad (16)$$

If the JSA is antisymmetric, i.e., $f(\omega_s, \omega_i) = -f(\omega_i, \omega_s)$, Eq.(13) can be further simplified as

$$R_A(\tau_0, \tau, \mu) = \frac{1}{2} \left(1 - \frac{1}{2} Re[F_+(\mu, 2\tau)] Re[P_-(\tau_0)] + \frac{1}{2} Re[F_+(\mu, 2\tau)] + \frac{1}{2} Re[e^{-i\mu\tau/2} F_-(\mu, 2\tau)] \right. \\ \left. + \frac{1}{4} Re[e^{-i\mu\tau/2} F_-(\mu, 2(\tau + \tau_0))] + \frac{1}{4} Re[e^{-i\mu\tau/2} F_-(\mu, 2(\tau - \tau_0))] \right). \quad (17)$$

where $P_-(\tau_0)$ has a similar definition as Eq.(15). Analogously, to distinguish two interferograms of last terms in Eq.(17), τ_0 must be much larger than the inverse linewidth $1/\sigma_-$, resulting in $Re[P_-(\tau_0)] \sim 0$. Thus, we have

$$R_A(\tau_0, \tau, \mu) = \frac{1}{2} \left(1 + \frac{1}{2} Re[F_+(\mu, 2\tau)] + \frac{1}{2} Re[e^{-i\mu\tau/2} F_-(\mu, 2\tau)] \right. \\ \left. + \frac{1}{4} Re[e^{-i\mu\tau/2} F_-(\mu, 2(\tau + \tau_0))] + \frac{1}{4} Re[e^{-i\mu\tau/2} F_-(\mu, 2(\tau - \tau_0))] \right). \quad (18)$$

Note that since the combination interferometer depends on both the frequency sum and difference between the signal and the idler photons for any symmetric JSA, it allows to measure simultaneously the amplitude of biphotons associated with both frequency sum and difference for symmetric JSA or antisymmetric JSA in a single quantum interferometer [20]. With the generalized combination interferometer, it is possible to measure simultaneously the real parts of F_+ and F_- associated with both frequency sum and difference for symmetric JSA (Eq.(16)) or antisymmetric JSA (Eq.(18)). If one introduces a phase $e^{i\pi/2}$ in one of the arms inside the generalized combination interferometer, then the imaginary part of F_+ and F_- are both measured. Once the real and imaginary parts are obtained, assuming that $f_{\pm}(0) = 0$, using the reconstruction formulas defined in Eq.(12), one can perform the full tomography of both f_+ and f_- for symmetric JSA or antisymmetric JSA. This has been shown schematically in the right part of Fig.1(c).

V. DISCUSSION

From Eq.(3) we can see that for the generalized HOM interferometer, the coincidence counts always depend on frequency difference of biphotons associated with the phase matching part f_- , whatever the JSA is symmetric, antisymmetric or anyonic. It thus only allows the measurement of the amplitude and phase of biphotons associated with frequency difference for any symmetric JSA, performing the partial tomography of biphotons.

From Eq.(7) and (9) we can see that for the generalized N00N state interferometer, the coincidence count rates depend on the frequency sum of biphotons for the symmetric JSA but the frequency difference for the antisymmetric JSA. There exists a one-to-one correspondence between coincidence count rates and F_+ for symmetric JSA (see Eq.(7) or F_- for antisymmetric JSA (see Eq.(9)). It means that the real or imaginary part of F_+ or F_- can be obtained directly from the coincidence data measured at different μ . It thus only allows the measurement of the amplitude and phase of biphotons associated with frequency sum for symmetric JSA or frequency difference for antisymmetric JSA, performing the partial tomography of biphotons, too.

For biphotons having an anyonic symmetry, it will result in an interference between the symmetric and the antisymmetric part associated with the phase matching part f_- in the generalized HOM interferometer, and an interference effect between the symmetric part associated with F_+ and the antisymmetric one associated with F_- in the generalized N00N state interferometer, owing to the frequency shift μ as discussed in [27]. It is thus impossible to perform simultaneously the full tomography of f_+ and f_- with these two generalized interferometers.

However, in a generalized combination interferometer, the coincidence count rates depend on both frequency sum and difference (see Eq.(16) and Eq.(18)) and have no one-to-one correspondence with F_+ or F_- but their mixture. In this case, it is necessary to postprocess the coincidence data to extract the wanted information of F_+ and F_- . For example, in Eq.(16), one needs to get first the real part of F_+ that contained in the total coincidence data. Because τ_0 must be much larger than the inverse linewidth $1/\sigma_+$, the coincidence data containing the last two terms in Eq.(16) is well distinguished from other parts. It is thus possible to extract the coincidence data associated with the real part of F_+ from the total the coincidence data. Then substituting the real part of F_+ into Eq.(16), one can obtain the real part of F_- indirectly. The imaginary parts of F_+ and F_- can be obtained in a similar manner. With both the real

and imaginary parts of F_+ and F_- , using the reconstruction formulas defined in Eq.(12), one can perform the full tomography of both f_+ and f_- for symmetric JSA. For antisymmetric JSA, the situation is analogous, where Eq.(18) can be used to perform the full tomography of both f_+ and f_- .

For biphotons having an anyonic symmetry, the coincidence count rates of the generalized combination interferometer will become more complex, and Eq.(16) and Eq.(18) do not hold yet. A possible way to solve this issue is that we can create a superposition state to satisfy the exchange symmetry condition, $\mathcal{F}_S(\omega_s, \omega_i) = f(\omega_s, \omega_i) + f(\omega_i, \omega_s)$, $\mathcal{F}_A(\omega_s, \omega_i) = f(\omega_s, \omega_i) - f(\omega_i, \omega_s)$, which are symmetric and antisymmetric, respectively. Experimentally, this can be realized by placing a nonlinear crystal inside an interferometer, as reported in [33]. Then, the information of biphotons with f_\pm might be extracted from the ones with \mathcal{F}_S or \mathcal{F}_A .

Experimentally, biphotons with symmetric, antisymmetric, or anyonic JSA can be generated by different methods [33–36]. On the other hand, the frequency shift can be realized experimentally by recent and promising electro-optics modulators [37, 38], or a waveguide-based optomechanical system based on piezoelectric effect [39]. Another way of implementing such a frequency shift for wider spectral distributions consists in introducing a dynamical shift of the eigenfrequencies or eigenmodes of optical resonators or waveguides [40], which corresponds to a tuning of the photon frequency. In a word, it is feasible to perform experimentally the full tomography of biphotons with the generalized combination interferometer after a careful choice for biphoton resource, frequency shift and experimental setup. If there is no frequency shift μ in generalized interferometers shown in Fig.(1), i.e., $\mu = 0$, they would come back to the original ones and only allow the measurement of the amplitude of the corresponding f [20].

VI. CONCLUSIONS

By introducing a frequency shift in one arm of interferometers, we describe theoretically three generalized quantum interferometers, i.e., the generalized HOM interferometer, the generalized N00N state interferometer and the generalized combination interferometer. It is found that the generalized HOM interferometer only allows the measurement of the amplitude and phase of biphotons associated with frequency difference for any symmetric JSA, while the N00N state interferometer allows the measurement of the amplitude and phase of biphotons associated with frequency sum for symmetric JSA or frequency difference for antisymmetric JSA. However, with the generalized combination interferometer, it is possible to measure the amplitude and phase of biphotons associated with both frequency sum and difference for symmetric JSA or antisymmetric JSA in a single interferometer. Considering an experimental feasibility to perform the full tomography of biphotons, a post-processing for the coincidence data measured at different frequency shifts may be required. This work provides an alternative method for full characterization of an arbitrary two-photon state with exchange symmetry and might become a useful tool for high-dimensional quantum information processing.

ACKNOWLEDGMENTS

This work has been supported by National Natural Science Foundation of China (12074309, 12074299, 12033007, 61875205, 12103058, 61801458), the Youth Innovation Team of Shaanxi Universities, and the Natural Science Foundation of Hubei Province (2022CFA039).

Appendix A: The coincidence count rates for a generalized HOM interferometer

For a generalized HOM interferometer as described in Fig. 1(a), the coincidence count rates between two detectors D1 and D2 as functions of the time delay τ and the frequency shift μ can be expressed as

$$R(\tau, \mu) = \frac{1}{2} \int \int d\omega_s d\omega_i \left| f(\omega_i + \mu, \omega_s) e^{-i\omega_s \tau} - f(\omega_s + \mu, \omega_i) e^{-i\omega_i \tau} \right|^2. \quad (\text{A1})$$

For a normalized $f(\omega_s, \omega_i)$, using the relations,

$$\begin{aligned} \omega_i + \mu - \omega_s &= 2[(\omega_i - \omega_s)/2 + \mu/2] = 2[\mu/2 - \omega_-], \\ \omega_s + \mu - \omega_i &= 2[(\omega_s - \omega_i)/2 + \mu/2] = 2[\mu/2 + \omega_-], \\ f(\omega_s, \omega_i) &= f_+(\omega_+) f_-(\omega_-); f(\omega_i, \omega_s) = -f_+(\omega_+) f_-(\omega_-). \end{aligned} \quad (\text{A2})$$

Eq. (A1) can be reduced to

$$\begin{aligned}
R(\tau, \mu) &= \frac{1}{4} \int \int d\omega_+ d\omega_- \left| f_+(\omega_+) f_-(\mu/2 - \omega_-) e^{-i(\omega_+ + \omega_-)\tau} - f_+(\omega_+) f_-(\mu/2 + \omega_-) e^{-i(\omega_+ - \omega_-)\tau} \right|^2 \\
&= \frac{1}{4} \int d\omega_+ |f_+(\omega_+)|^2 \int d\omega_- \left| f_-(\mu/2 - \omega_-) e^{-i\omega_- \tau} - f_-(\mu/2 + \omega_-) e^{i\omega_- \tau} \right|^2 \\
&= \frac{1}{4} \int d\omega_- \left| f_-(\mu/2 - \omega_-) e^{-i\omega_- \tau} - f_-(\mu/2 + \omega_-) e^{i\omega_- \tau} \right|^2 \\
&= \frac{1}{4} \int d\omega_- \left(f_-(\mu/2 - \omega_-) e^{-i\omega_- \tau} - f_-(\mu/2 + \omega_-) e^{i\omega_- \tau} \right) \left(f_-(\mu/2 - \omega_-) e^{-i\omega_- \tau} - f_-(\mu/2 + \omega_-) e^{i\omega_- \tau} \right)^* \\
&= \frac{1}{4} \int d\omega_- \left(|f_-(\mu/2 - \omega_-)|^2 + |f_-(\mu/2 + \omega_-)|^2 \right. \\
&\quad \left. - f_-(\mu/2 - \omega_-) f_+^*(\mu/2 + \omega_-) e^{-i2\omega_- \tau} - f_+^*(\mu/2 - \omega_-) f_-(\mu/2 + \omega_-) e^{i2\omega_- \tau} \right) \\
&= \frac{1}{2} \left(1 - \text{Re}[W_-(\tau, \mu/2)] \right). \tag{A3}
\end{aligned}$$

where W_- is the chronocyclic Wigner distribution of the phase matching function f_- as defined in Eq.(4). In above derivation, we change the variables in the double integral from ω_s, ω_i to ω_+, ω_- , and use the normalized condition, i.e., $\int d\omega_+ |f_+(\omega_+)|^2 = \int d\omega_- |f_-(\mu/2 - \omega_-)|^2 = \int d\omega_- |f_-(\mu/2 + \omega_-)|^2 = 1$.

Appendix B: The coincidence count rates for a generalized N00N state interferometer

For a generalized N00N state interferometer as described in Fig. 1(b), the coincidence count rates between two detectors D3 and D4 as functions of the time delay τ and the frequency shift μ can be expressed as

$$R(\tau, \mu) = \frac{1}{2} \int \int d\omega_s d\omega_i \left| f(\omega_s, \omega_i, \mu) (e^{-i(\omega_s + \mu)\tau} + 1) (e^{-i(\omega_i + \mu)\tau} + 1) + f(\omega_i, \omega_s, \mu) (e^{-i(\omega_i + \mu)\tau} - 1) (e^{-i(\omega_s + \mu)\tau} - 1) \right|^2. \tag{B1}$$

If the JSA is symmetric, i.e., $f(\omega_s, \omega_i) = f(\omega_i, \omega_s)$, we can further simplify Eq.(B1) as

$$\begin{aligned}
R_S(\tau, \mu) &= \frac{1}{2} \int \int d\omega_s d\omega_i \left| f(\omega_s + \mu, \omega_i + \mu) + f(\omega_s, \omega_i) e^{i(\omega_s + \omega_i + 2\mu)\tau} \right|^2 \\
&= \frac{1}{2} \int \int d\omega_s d\omega_i \left(f(\omega_s + \mu, \omega_i + \mu) + f(\omega_s, \omega_i) e^{i(\omega_s + \omega_i + 2\mu)\tau} \right) \left(f(\omega_s + \mu, \omega_i + \mu) + f(\omega_s, \omega_i) e^{i(\omega_s + \omega_i + 2\mu)\tau} \right)^* \\
&= \frac{1}{2} \int \int d\omega_s d\omega_i \left(|f(\omega_s + \mu, \omega_i + \mu)|^2 + |f(\omega_s, \omega_i)|^2 \right. \\
&\quad \left. + f(\omega_s, \omega_i) f^*(\omega_s + \mu, \omega_i + \mu) e^{i(\omega_s + \omega_i + 2\mu)\tau} + f^*(\omega_s, \omega_i) f(\omega_s + \mu, \omega_i + \mu) e^{-i(\omega_s + \omega_i + 2\mu)\tau} \right). \tag{B2}
\end{aligned}$$

For a normalized $f(\omega_s, \omega_i)$, using the relations,

$$\begin{aligned}
\omega_s + \mu + (\omega_i + \mu) &= 2[(\omega_s + \omega_i)/2 + \mu] = 2(\omega_+ + \mu), \\
\omega_s + \mu - (\omega_i + \mu) &= 2[(\omega_s - \omega_i)/2] = 2\omega_-, \\
f(\omega_s, \omega_i) &= f_+(\omega_+) f_-(\omega_-); f(\omega_s + \mu, \omega_i + \mu) = f_+(\omega_+ + \mu) f_-(\omega_-). \tag{B3}
\end{aligned}$$

Eq. (B2) can be reduced to

$$\begin{aligned}
R_S(\tau, \mu) &= \frac{1}{4} \int \int |f_-(\omega_-)|^2 d\omega_- d\omega_+ \left(|f_+(\omega_+ + \mu)|^2 + |f_+(\omega_+)|^2 \right. \\
&\quad \left. + f_+(\omega_+) f^*(\omega_+ + \mu) e^{i(2\omega_+ + \mu)\tau} + f_+^*(\omega_+) f_+(\omega_+ + \mu) e^{-i(2\omega_+ + \mu)\tau} \right) \\
&= \frac{1}{2} \left(1 + \text{Re}[F_+(\mu, 2\tau)] \right). \tag{B4}
\end{aligned}$$

where F_+ is the STFT of the function f_+ as defined in Eq.(8). In above derivation, we change the variables in the double integral from ω_s, ω_i to ω_+, ω_- , and use the normalized condition, i.e., $\int d\omega_- |f_-(\omega_-)|^2 = \int d\omega_+ |f_+(\omega_+ + \mu)|^2 = \int d\omega_+ |f_+(\omega_+)|^2 = 1$.

If the JSA is antisymmetric, i.e., $f(\omega_s, \omega_i) = -f(\omega_i, \omega_s)$, we can further simplify Eq.(B1) as

$$\begin{aligned}
R_A(\tau, \mu) &= \frac{1}{2} \int \int d\omega_s d\omega_i \left| f(\omega_s + \mu, \omega_i) e^{-i\omega_s \tau} + f(\omega_s, \omega_i + \mu) e^{-i\omega_i \tau} \right|^2 \\
&= \frac{1}{2} \int \int d\omega_s d\omega_i \left(f(\omega_s + \mu, \omega_i) e^{-i\omega_s \tau} + f(\omega_s, \omega_i + \mu) e^{-i\omega_i \tau} \right) \left(f(\omega_s + \mu, \omega_i) e^{-i\omega_s \tau} + f(\omega_s, \omega_i + \mu) e^{-i\omega_i \tau} \right)^* \\
&= \frac{1}{2} \int \int d\omega_s d\omega_i \left(|f(\omega_s + \mu, \omega_i)|^2 + |f(\omega_s, \omega_i + \mu)|^2 \right. \\
&\quad \left. + f(\omega_s + \mu, \omega_i) f^*(\omega_s, \omega_i + \mu) e^{-i(\omega_s - \omega_i)\tau} + f^*(\omega_s + \mu, \omega_i) f(\omega_s, \omega_i + \mu) e^{i(\omega_s - \omega_i)\tau} \right). \tag{B5}
\end{aligned}$$

For a normalized $f(\omega_s, \omega_i)$, using the relations,

$$\begin{aligned}
\omega_s - (\omega_i + \mu) &= 2[(\omega_s + \omega_i)/2 - \mu/2] = 2(\omega_- - \mu/2), \\
(\omega_s + \mu) - \omega_i &= 2[(\omega_s - \omega_i)/2 + \mu/2] = 2(\omega_+ + \mu/2), \\
f(\omega_s + \mu, \omega_i) &= f_+(\omega_+ + \mu/2) f_-(\omega_- + \mu/2); \\
f(\omega_s, \omega_i + \mu) &= f_+(\omega_+ + \mu/2) f_-(\omega_- - \mu/2). \tag{B6}
\end{aligned}$$

Eq. (B5) can be reduced to

$$\begin{aligned}
R_A(\tau, \mu) &= \frac{1}{4} \int \int |f_+(\omega_+ + \mu/2)|^2 d\omega_+ d\omega_- \left(|f_-(\omega_- + \mu/2)|^2 + |f_-(\omega_- - \mu/2)|^2 \right. \\
&\quad \left. + f_-(\omega_- - \mu/2) f^*_-(\omega_- + \mu/2) e^{-i(2\omega_-)\tau} + f^*_-(\omega_- - \mu/2) f_-(\omega_- + \mu/2) e^{i(2\omega_-)\tau} \right) \\
&= \frac{1}{2} \left(1 + \text{Re}[e^{-i\mu\tau/2} F_-(\mu, 2\tau)] \right). \tag{B7}
\end{aligned}$$

where F_- is the STFT of the function f_- as defined in Eq.(10). In above derivation, we change the variables in the double integral from ω_s, ω_i to ω_+, ω_- , and use the normalized condition, i.e., $\int d\omega_+ |f_+(\omega_+ + \mu/2)|^2 = \int d\omega_- |f_-(\omega_- + \mu/2)|^2 = \int d\omega_- |f_-(\omega_- - \mu/2)|^2 = 1$.

Appendix C: The coincidence count rates for a generalized combination interferometer

For a generalized combination interferometer as described in Fig. 1(c), the coincidence count rates between two detectors D5 and D6 as functions of the time delay τ and the frequency shift μ can be expressed as

$$\begin{aligned}
R(\tau_0, \tau, \mu) &= \frac{1}{64} \int \int d\omega_s d\omega_i \\
&\times \left| f(\omega_s, \omega_i, \mu) (e^{-i\omega_s \tau_0} e^{-i(\omega_s + \mu)\tau} + e^{-i\omega_s \tau_0} + e^{-i(\omega_s + \mu)\tau} - 1) (e^{-i\omega_i \tau_0} e^{-i(\omega_i + \mu)\tau} - e^{-i\omega_i \tau_0} - e^{-i(\omega_i + \mu)\tau} - 1) \right. \\
&\quad \left. + f(\omega_i, \omega_s, \mu) (e^{-i\omega_i \tau_0} e^{-i(\omega_i + \mu)\tau} + e^{-i(\omega_i + \mu)\tau} - e^{-i\omega_i \tau_0} + 1) (e^{-i\omega_s \tau_0} e^{-i(\omega_s + \mu)\tau} - e^{-i(\omega_s + \mu)\tau} + e^{-i\omega_s \tau_0} + 1) \right|^2 \tag{C1}
\end{aligned}$$

To simplify the expressions, we use $f_{(\omega_s, \omega_i)}$ to denote $f(\omega_s, \omega_i)$, others similarly, in the following derivations. If the JSA is symmetric, i.e., $f_{(\omega_s, \omega_i)} = f_{(\omega_i, \omega_s)}$, we can further simplify Eq.(C1) as

$$\begin{aligned}
R_S(\tau_0, \tau, \mu) &= \frac{1}{64} \int \int d\omega_s d\omega_i \\
&\times \left| f_{(\omega_s, \omega_i)} - f_{(\omega_s + \mu, \omega_i)} e^{-i(\omega_s + \mu)\tau} + f_{(\omega_s, \omega_i + \mu)} e^{-i(\omega_i + \mu)\tau} - f_{(\omega_s, \omega_i)} e^{-i(\omega_s + \omega_i)\tau_0} - f_{(\omega_s + \mu, \omega_i)} e^{-i(\omega_s + \mu)\tau} e^{-i(\omega_s + \omega_i)\tau_0} \right. \\
&\quad \left. - f_{(\omega_s + \mu, \omega_i + \mu)} e^{-i(\omega_s + \omega_i + 2\mu)\tau} + f_{(\omega_s, \omega_i + \mu)} e^{-i(\omega_i + \mu)\tau} e^{-i(\omega_s + \omega_i)\tau_0} + f_{(\omega_s + \mu, \omega_i + \mu)} e^{-i(\omega_s + \omega_i + 2\mu)\tau} e^{-i(\omega_s + \omega_i)\tau_0} \right|^2 \\
&= \frac{1}{64} \int \int d\omega_s d\omega_i \\
&\times \left\{ 8 \left(|f_{(\omega_s, \omega_i)}|^2 + |f_{(\omega_s + \mu, \omega_i)}|^2 + |f_{(\omega_s, \omega_i + \mu)}|^2 + |f_{(\omega_s + \mu, \omega_i + \mu)}|^2 \right) \right. \\
&\quad \left. - 4 \left(f_{(\omega_s + \mu, \omega_i)} f^*_{(\omega_s, \omega_i + \mu)} e^{-i(\omega_s - \omega_i)\tau} + f^*_{(\omega_s + \mu, \omega_i)} f_{(\omega_s, \omega_i + \mu)} e^{i(\omega_s - \omega_i)\tau} \right) \times \left(f_{(\omega_s, \omega_i)} e^{-i(\omega_s + \omega_i)\tau_0} + f^*_{(\omega_s, \omega_i)} e^{i(\omega_s + \omega_i)\tau_0} \right) \right\}
\end{aligned}$$

$$\begin{aligned}
& -8 \left(f_{(\omega_s+\mu, \omega_i+\mu)} f_{(\omega_s+\mu, \omega_i+\mu)}^* e^{-i(\omega_s+\omega_i+2\mu)\tau} + f_{(\omega_s+\mu, \omega_i+\mu)}^* f_{(\omega_s+\mu, \omega_i+\mu)} e^{i(\omega_s+\omega_i+2\mu)\tau} \right) \\
& -8 \left(f_{(\omega_s+\mu, \omega_i)} f_{(\omega_s, \omega_i+\mu)}^* e^{-i(\omega_s-\omega_i)\tau} + f_{(\omega_s+\mu, \omega_i)}^* f_{(\omega_s, \omega_i+\mu)} e^{i(\omega_s-\omega_i)\tau} \right) \\
& +4 \left(f_{(\omega_s+\mu, \omega_i)} f_{(\omega_s, \omega_i+\mu)}^* e^{-i(\omega_s+\omega_i)\tau_0} e^{i(\omega_s+\omega_i+2\mu)\tau} + f_{(\omega_s+\mu, \omega_i)}^* f_{(\omega_s, \omega_i+\mu)} e^{i(\omega_s+\omega_i)\tau_0} e^{-i(\omega_s+\omega_i+2\mu)\tau} \right) \\
& +4 \left(f_{(\omega_s+\mu, \omega_i)} f_{(\omega_s, \omega_i+\mu)}^* e^{-i(\omega_s+\omega_i)\tau_0} e^{-i(\omega_s+\omega_i+2\mu)\tau} + f_{(\omega_s+\mu, \omega_i)}^* f_{(\omega_s, \omega_i+\mu)} e^{i(\omega_s+\omega_i)\tau_0} e^{i(\omega_s+\omega_i+2\mu)\tau} \right) \}. \quad (C2)
\end{aligned}$$

For a normalized $f(\omega_s, \omega_i)$, using Eq.(B3) and Eq.(B6), Eq.(C2) can be reduced to

$$\begin{aligned}
R_S(\tau_0, \tau, \mu) = & \frac{1}{2} \left\{ 1 - \frac{1}{64} \int |f_{\omega_+}|^2 d\omega_+ \int d\omega_- \right. \\
& + \left\{ 4 \left(f_{(\omega_-+\mu/2, \omega_--\mu/2)} f_{(\omega_-+\mu/2, \omega_--\mu/2)}^* e^{-i2\omega_- \tau} + f_{(\omega_-+\mu/2, \omega_--\mu/2)}^* f_{(\omega_-+\mu/2, \omega_--\mu/2)} e^{i2\omega_- \tau} \right) \right. \\
& \times \left(f_{\omega_+} e^{-i(2\omega_++2\mu)\tau_0} + f_{\omega_+}^* e^{i(2\omega_++2\mu)\tau_0} \right) \\
& + 8 \left(f_{(\omega_+, \omega_++\mu)} f_{(\omega_+, \omega_++\mu)}^* e^{-i(2\omega_++2\mu)\tau} + f_{(\omega_+, \omega_++\mu)}^* f_{(\omega_+, \omega_++\mu)} e^{i(2\omega_++2\mu)\tau} \right) \\
& + 8 \left(f_{(\omega_-+\mu/2, \omega_--\mu/2)} f_{(\omega_-+\mu/2, \omega_--\mu/2)}^* e^{-i2\omega_- \tau} + f_{(\omega_-+\mu/2, \omega_--\mu/2)}^* f_{(\omega_-+\mu/2, \omega_--\mu/2)} e^{i2\omega_- \tau} \right) \\
& - 4 \left(f_{(\omega_+, \omega_++\mu)} f_{(\omega_+, \omega_++\mu)}^* e^{-i(2\omega_++2\mu)\tau_0} e^{-i(2\omega_++2\mu)\tau} + f_{(\omega_+, \omega_++\mu)}^* f_{(\omega_+, \omega_++\mu)} e^{i(2\omega_++2\mu)\tau_0} e^{i(2\omega_++2\mu)\tau} \right) \\
& \left. \left. - 4 \left(f_{(\omega_+, \omega_++\mu)} f_{(\omega_+, \omega_++\mu)}^* e^{-i(2\omega_++2\mu)\tau_0} e^{i(2\omega_++2\mu)\tau} + f_{(\omega_+, \omega_++\mu)}^* f_{(\omega_+, \omega_++\mu)} e^{i(2\omega_++2\mu)\tau_0} e^{-i(2\omega_++2\mu)\tau} \right) \right\} \right\}. \quad (C3)
\end{aligned}$$

In above derivation, we change the variables in the double integral from ω_s, ω_i to ω_+, ω_- , and use the normalized condition, i.e., $\int d\omega_- |f_-(\omega_-)|^2 = \int d\omega_+ |f_+(\omega_+)|^2 = \int d\omega_+ |f_+(\omega_++\mu/2)|^2 = \int d\omega_+ |f_+(\omega_+-\mu/2)|^2 = \int d\omega_- |f_-(\omega_-+\mu/2)|^2 = \int d\omega_- |f_-(\omega_--\mu/2)|^2 = 1$. Finally, we arrive at

$$\begin{aligned}
R_S(\tau_0, \tau, \mu) = & \frac{1}{2} \left(1 - \frac{1}{2} \text{Re}[e^{-i\mu\tau/2} F_-(\mu, 2\tau)] \text{Re}[P_+(\tau_0)] - \frac{1}{2} \text{Re}[F_+(\mu, 2\tau)] - \frac{1}{2} \text{Re}[e^{-i\mu\tau/2} F_-(\mu, 2\tau)] \right. \\
& \left. + \frac{1}{4} \text{Re}[F_+(\mu, 2(\tau + \tau_0))] + \frac{1}{4} \text{Re}[F_+(\mu, 2(\tau - \tau_0))] \right). \quad (C4)
\end{aligned}$$

where F_+ and F_- are the STFT of the function f_+ and f_- , respectively, as defined in Eq.(8) and Eq.(10). If the JSA is antisymmetric, i.e., $f_{(\omega_s, \omega_i)} = -f_{(\omega_i, \omega_s)}$, the derivation process is similar and we give directly the results as follows,

$$\begin{aligned}
R_A(\tau_0, \tau, \mu) = & \frac{1}{2} \left(1 - \frac{1}{2} \text{Re}[F_+(\mu, 2\tau)] \text{Re}[P_-(\tau_0)] + \frac{1}{2} \text{Re}[F_+(\mu, 2\tau)] + \frac{1}{2} \text{Re}[e^{-i\mu\tau/2} F_-(\mu, 2\tau)] \right. \\
& \left. + \frac{1}{4} \text{Re}[e^{-i\mu\tau/2} F_-(\mu, 2(\tau + \tau_0))] + \frac{1}{4} \text{Re}[e^{-i\mu\tau/2} F_-(\mu, 2(\tau - \tau_0))] \right). \quad (C5)
\end{aligned}$$

where $P_-(\tau_0)$ has a similar expression as defined in Eq.(15).

[1] J. M. Lukens and P. Lougovski, "Frequency-encoded photonic qubits for scalable quantum information processing," *Optica* **4**(1), 8-16 (2017).

[2] C. Reimer, S. Sciara, P. Roztocki, M. Islam, L. R. Cortés, Y. Zhang, B. Fischer, S. Loranger, R. Kashyap, A. Cino, S. T. Chu, B. E. Little, D. J. Moss, L. Caspani, W. J. Munro, J. Azaña, M. Kues, and R. Morandotti, "High-dimensional one-way quantum processing implemented on d-level cluster states," *Nat. Phys.* **15**(2), 148-153 (2019).

[3] Chi, Y., Yu, Y., Gong, Q. et al, "High-dimensional quantum information processing on programmable integrated photonic chips," *Sci. China Inf. Sci.* **66**, 180501 (2023).

[4] Ali-Khan, I., Broadbent, C. J. and Howell, J. C., "Large-alphabet quantum key distribution using energy-time entangled bipartite states," *Phys. Rev. Lett.* **98**, 060503 (2007).

[5] J. Nunn, L. J. Wright, C. Söller, L. Zhang, I. A. Walmsley, and B. J. Smith, "Large-alphabet time-frequency entangled quantum key distribution by means of time-to-frequency conversion," *Opt. Express* **17**, 15959-15973 (2013).

[6] Tian Zhong et al, "Photon-efficient quantum key distribution using time-energy entanglement with high-dimensional encoding," *New J. Phys.* **17** 022002 (2015).

[7] V. Giovannetti, S. Lloyd, and L. Maccone, "Advances in quantum metrology," *Nat. Photonics* **5**, 222-229 (2011).

[8] Lanyon, B. P. et al. "Simplifying quantum logic using higher-dimensional Hilbert spaces," *Nat. Phys.* **5**, 134-140 (2009)

[9] Kevin Zielnicki, Karina Garay-Palmett, Daniel Cruz-Delgado, Hector Cruz-Ramirez, Michael F. O'Boyle, Bin Fang, Virginia O. Lorenz, Alfred B. U'Ren and Paul G. Kwiat, "Joint spectral characterization of photon-pair sources," *Journal of Modern Optics* **65**:10, 1141-1160 (2018).

[10] O. Kuzucu, F. N. Wong, S. Kurimura, and S. Tovstonog, "Joint temporal density measurements for two-photon state characterization," *Phys. Rev. Lett.* **101**, 153602 (2008).

[11] J.-P. W. MacLean, J. M. Donohue, and K. J. Resch, "Direct characterization of ultrafast energy-time entangled photon pairs," *Phys. Rev. Lett.* **120**, 053601 (2018).

[12] Rui-Bo Jin, and Ryosuke Shimizu, "Extended Wiener-Khinchin theorem for quantum spectral analysis," *Optica* **5**, 93-98 (2018).

[13] Hiroya Seki, Kensuke Miyajima, and Ryosuke Shimizu, "Quantum interferometric spectroscopy of a biexciton," *Phys. Rev. A* **106**, 063716 (2022).

[14] Chen Y, Chen L, "Quantum Wiener-Khinchin Theorem for Spectral-Domain Optical Coherence Tomography," *Phys. Rev. Applied* **18**, 014077 (2022).

[15] C. K. Hong, Z. Y. Ou, and L. Mandel, "Measurement of subpicosecond time intervals between two photons by interference," *Phys. Rev. Lett.* **59**, 2044-2046 (1987).

[16] Frédéric Bouchard, Alicia Sit, Yingwen Zhang, Robert Fickler, Filippo M Miatto, Yuan Yao, Fabio Sciarrino and Ebrahim Karimi, "Two-photon interference: the Hong-Ou-Mandel effect," *Rep. Prog. Phys.* **84**, 012402 (2021).

[17] A. N. Boto, P. Kok, D. S. Abrams, S. L. Braunstein, C. P. Williams, and J. P. Dowling, "Quantum Interferometric Optical Lithography: Exploiting Entanglement to Beat the Diffraction Limit," *Phys. Rev. Lett.* **85**, 2733 (2000).

[18] Y. Israel, S. Rosen, and Y. Silberberg, "Supersensitive polarization microscopy using NOON states of light," *Phys. Rev. Lett.* **112**, 103604(2014).

[19] M. Bergmann and P. van Loock, "Quantum error correction against photon loss using noon states," *Phys. Rev. A* **94**, 012311 (2016).

[20] Baihong Li, Changhua Chen, Xiao Xiang, Runai Quan, Ruifang Dong, Shougang Zhang, Xiangying Hao, and Rui-Bo Jin, "Complete spectral characterization of biphotons by simultaneously determining their frequency sum and difference in a single quantum interferometer", *Phys. Rev. A* **108**, 023713 (2023).

[21] Rui-Bo Jin, Takuma Saito, and Ryosuke Shimizu, "Time-Frequency Duality of Biphotons for Quantum Optical Synthesis," *Phys. Rev. Applied* **10**, 034011 (2018).

[22] Jean-Philippe W. MacLean, Sacha Schwarz, and Kevin J. Resch, "Reconstructing ultrafast energy-time-entangled two-photon pulses," *Phys. Rev. A* **100**, 033834(2019).

[23] I. Gianani, "Robust spectral phase reconstruction of time-frequency entangled bi-photon states," *Phys. Rev. Research* **1**, 033165 (2019)

[24] Alex O. C. Davis, Valérian Thiel, and Brian J. Smith, "Measuring the quantum state of a photon pair entangled in frequency and time," *Optica* **7**, 1317-1322 (2020)

[25] I. Gianani, M. Sbroscia, and M. Barbieri, "Measuring the time-frequency properties of photon pairs: A short review," *AVS Quantum Science*, **2**, 011701 (2020)

[26] Michał Karpiński, Alex O. C. Davis, Filip Sośnicki, Valérian Thiel, and Brian J. Smith, "Control and Measurement of Quantum Light Pulses for Quantum Information Science and Technology," *Adv. Quantum Technol.* **4**, 2000150 (2021)

[27] Fabre, N., "Interferometric signature of different spectral symmetries of biphoton states," *Phys. Rev. A* **105**, 053716 (2022).

[28] T. Douce, A. Eckstein, S. P. Walborn, A. Z. Khoury, S. Ducci, A. Keller, T. Coudreau, and P. Milman, "Direct measurement of the biphoton Wigner function through two-photon interference", *Sci. Rep.* **3**, 3530 (2013).

[29] G. Boucher, T. Douce, D. Bresteau, S. P. Walborn, A. Keller, T. Coudreau, S. Ducci, and P. Milman, "Toolbox for continuous-variable entanglement production and measurement using spontaneous parametric down-conversion," *Phys. Rev. A* **92**, 023804 (2015).

[30] A. Eckstein and C. Silberhorn, "Broadband frequency mode entanglement in waveguided parametric downconversion," *Opt. Lett.* **33**, 1825-1827 (2008).

[31] N. Fabre, G. Maltese, F. Appas, S. Felicetti, A. Ketterer, A. Keller, T. Coudreau, F. Baboux, M. I. Amanti, S. Ducci, and P. Milman, "Generation of a time-frequency grid state with integrated biphoton frequency combs", *Phys. Rev. A* **102**, 012607 (2020).

[32] Vittorio Giovannetti, Lorenzo Maccone, Jeffrey H. Shapiro, and Franco N. C. Wong, "Extended phase-matching conditions for improved entanglement generation," *Phys. Rev. A* **66**, 043813 (2002).

[33] R.-B. Jin, R. Shiina, and R. Shimizu, "Quantum manipulation of biphoton spectral distributions in a 2D frequency space toward arbitrary shaping of a biphoton wave packet," *Opt. Express* **26**, 21153-21158 (2018).

[34] S. Francesconi, A. Raymond, N. Fabre, A. Lemaître, M. I. Amanti, P. Milman, F. Baboux, and S. Ducci, "Anyonic Two-Photon Statistics with a Semiconductor Chip," *ACS Photonics*, **9**, 2764-2769 (2021)

[35] L. Sansoni, F. Sciarrino, G. Vallone, P. Mataloni, A. Crespi, R. Ramponi, and R. Osellame, "Two-Particle Bosonic-Fermionic Quantum Walk via Integrated Photonics," *Phys. Rev. Lett.* **108**, 010502 (2012).

[36] S. Francesconi, F. Baboux, A. Raymond, N. Fabre, G. Boucher, A. Lemaître, P. Milman, M. Amanti, and S. Ducci, "Engineering two-photon wavefunction and exchange statistics in a semiconductor chip," *Optica* **7**, 316 (2020).

[37] Y. Hu, M. Yu, D. Zhu, N. Sinclair, A. Shams-Ansari, L. Shao, J. Holzgrafe, E. Puma, M. Zhang, and M. Lončar, "On-chip electro-optic frequency shifters and beam splitters," *Nature* **599**, 587 (2021).

[38] C. Chen, J. E. Heyes, J. H. Shapiro, and F. N. C. Wong, "Single-photon frequency shifting with a quadrature phase-shift keying modulator," *Sci. Rep.* **11**, 300 (2021).

[39] L. Fan, C.-L. Zou, M. Poot, R. Cheng, X. Guo, X. Han, and H. X. Tang, "Integrated optomechanical single-photon

frequency shifter”, Nat. Photonics **10**, 766 (2016).
[40] E. Kuramochi and M. Notomi, “Single-photon frequency shifting”, Nat. Photonics **10**, 752 (2016).